Transactions of the Materials Research Society of Japan 32[1] 297-302 (2007)

Evaluation of Small Ion Distribution in the Polyelectrolyte Brush at the Air/Water Interface by Neutron Reflectometry

Hideki Matsuoka, Emiko Mouri*, Ploysai Kaewsaiha, Yasuyuki Furuya, Yoshiko Suetomi, Kozo Matsumoto** and Noaya Torikai***

Department of Polymer Chemistry, Kyoto University, Kyoto 615-8510, Japan
Fax: 81-75-383-2599, e-mail: matsuoka@star.polym.kyoto-u.ac.jp
*Present Address: Department of Applied Chemistry, Kyushu Institute of Technology, Kitakyushu 804-8550, Japan
** Present Address: Molecular Engineering Institute (MEI), Kinki University, 11-6 Kayanomori Iizuka, Fukuoka, 820-8555, Japan
***Neutron Science Laboratory, High Energy Accelerator Research Organization, 1-1 Oho, Tsukuba, Ibaraki 305-0801, Japan

Cl^- ion distribution in the polyelectrolyte brush in the amphiphilic diblock copolymer monolayer on the water surface was evaluated by in situ neutron reflectivity (NR) technique with contrast variation method. The X-ray reflectivity (XR) profiles for spread monolayer of poly(diethylsilacyclobutane)-*b*-poly(methacrylic acid) with NaCl and NaBr as an added salt were well reproduced by 3-box model with assuming hydrophobic, carpet and brush triple layer structure. However, NR profile for 1M NaCl condition could not fitted by 3-box model while those for NaBr and NaCl at lower concentration could be fitted. NR profile under 1M NaCl condition with $D_2O/H_2O(8/2)$ as subphase, where the contribution from Cl^- ions to neutron reflectivity is eliminated, was well fitted with 3-box model with the same nanostructure of monolayer by XR. Hence, we concluded that the disagreement observed for 1M NaCl condition is due to the contribution of Cl^- ions whose distribution is inhomogeneous in brush layer. By model fitting of NR profile with inhomogeneous Cl^- ion distribution, it was predicted that Cl^- ions were concentrated just beneath the carpet layer.

Key words: Polyelectrolyte Brush, Neutron Reflectivity, Air/Water Interface, Small Ion Distribution, Contrast Variation

1. INTRODUCTION

When ionic amphiphilic diblock copolymers, which consist of hydrophobic blocks and polyelectrolyte chains, are spread on the water surface, they self-assemble to a polymer monolayer.[1-5] The hydrophilic block, i.e., polyelectrolyte segment, is expected to form a polyelectrolyte brush under the water surface, but it has been clarified that the nanostructure of hydrophilic layer in the polymer monolayer is not simple. [6-15] When a polyelectrolyte brush is formed, the so-called "carpet layer" is certainly formed between the hydrophobic layer on the water and the polyelectrolyte brush layer under the water surface. Hence, the monolayer has a triple layered structure consisting of hydrophobic, carpet and brush layers. Although the hydrophobic / brush double layered structure has never been observed, the hydrophobic / carpet double layered structure is often found. This situation is schematically shown in Figure 1. The required condition for formation of each layer has also been clarified; the brush layer appears only when the hydrophilic chain length is sufficiently long [7], when the brush density (the number of hydrophilic segments in a unit area, which is comparable to surface pressure for monolayer systems) is high enough [13,14], and also when the added salt concentration is sufficiently low [11]. Furthermore, the critical condition of these parameters where transition between these two structures (double layer and triple layer) occurs, has also been quantitatively investigated.

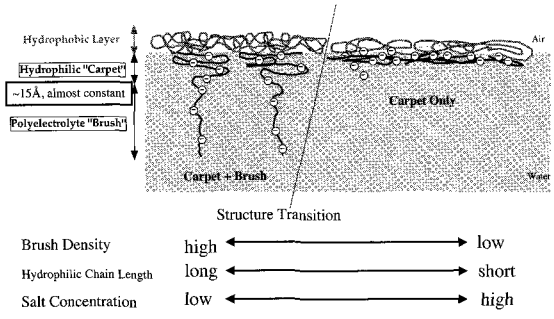

Fig. 1 Schematic representation of nanostructure and transition of ionic amphiphilic diblock copolymer monolayer on the water surface

In our previous studies, we applied X-ray reflectivity (XR) and neutron reflectivity (NR) techniques comprehensively as a unique technique to study the nanostructure of monolayer on the water surface directly. [7-15] By following common analysis method, we fitted the XR and NR profiles obtained by 2- or 3-box model to evaluate the density (electron density for X-ray, scattering length density for neutron) profile normal to the surface.

Most of all the XR and NR profiles were well fitted by the box model assuming that hydrophobic, carpet layers, and a brush layer exist. However, we have

noticed that some of the NR profiles with a rather high NaCl concentration as an added salt to water (D_2O) subphase could not be fitted by the 3-box model, while those with NaBr at the same concentration could be. Considering the difference of scattering length density between D_2O and Cl^- and between D_2O and Br^- ions, and also the fact that XR profiles in the same conditions were all well fitted by 3-box model, we thought that unsuccessful fitting of the NR profile in a high NaCl condition is due to the contribution of Cl^- ions in the brush layer which might be distributed inhomogeneously. In this study, we have proved this hypothesis by applying contrast variation NR measurements to eliminate the contribution from Cl^- of ions. Furthermore, by a fitting taking Cl^- ion distribution in the brush layer into account, a possibility that Cl^- ions are concentrated just below carpet layer has been suggested.

2.EXPERIMENTAL

2.1 Materials

The ionic amphiphilic diblock copolymer used in this study was poly(diethylsilacyclobutane)-*b*-poly(methacrylic acid) (poly(Et_2SB-d_{10})$_m$-*b*-poly(MAA)$_n$), which was synthesized as previously reported. [16] The hydrophobic chain was partly deuterated, and the degree of polymerization of the hydrophobic (m) and hydrophilic (n) block were m:n=23:49. This polymer is the same as that used in our previous study [8] and the polydispersity, M_w/M_n was 1.05.

2.2 XR and NR instruments and analyses

The XR instrument used was a RINT-TTR-MA system, whose details have been reported separately [17]. The NR instrument was an ARISA reflectometer, whose details were also described elsewhere [18] Both of these reflectometers have a sample horizontal optical geometry and have the Langmuir-Brodgett (LB) trough at the sample position to perform *in situ* measurements for the monolayer on the water. The data analysis method including fitting procedure and accuracy was the same as in our previous studies and has been described elsewhere [9,19]. For NR data analysis, we used SURFace software. Parratt32 was used for brush roughness analysis. We assumed 2.69×10^{-6}Å^{-2} and 4.91×10^{-6}Å^{-2} as the scattering length density values (Nb) for Br^- and Cl^- ions, respectively, which were calculated from their scattering length and ion radius. The scattering vector was represented by q and Q for XR and NR, respectively.

3.RESULTS AND DISCUSSION

3.1 Effect of NaCl addition

The effect of NaCl addition to water subphase for poly(Et_2SB)-*b*-poly(MAA) monolayer system was duly investigated by XR and NR in our previous study. [8] The result was in principle in agreement qualitatively with previous theoretical studies. [20-23] NaCl concentration was changed from 0M up to 1M, and what was interesting was the observation of expanding-shrinking behavior of the monolayer with increasing salt concentration. This curious phenomenon at first glance was interpreted by the balance of effective degree of dissociation of carboxylic acid and the shielding effect of salt ions on the electrostatic repulsion between polyelectrolyte brush chains. [8] The change of roughness of the brush layer was also interesting behavior. The brush top roughness increased with increasing NaCl concentration and showed the maximum at 0.1M NaCl condition, and then decreased. NR profiles for the monolayer at various NaCl concentrations were shown in Figure 2. The profiles were in principle the same as those in our previous study.[8] All the XR profiles measured could be analyzed by the 3-box model fitting. For NR profiles, those at low NaCl concentrations were well fitted by 3-box model and gave us the same nanostructure as XR results. However, that under 1M NaCl condition could not be fitted by the 3-box model fitting. (Hence, no fitting curve for curve 4 in Figure 2). On the other hand, XR profiles were well analyzed by the 3-box model up to a 2M NaCl condition[8]. This apparent disagreement between XR and NR data was a paradox.

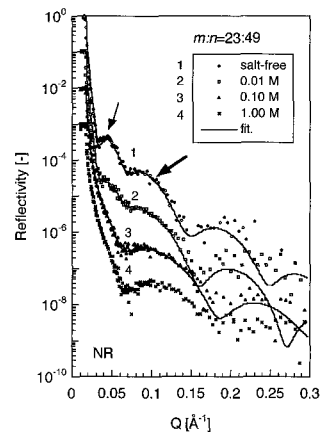

Fig. 2 NR profiles for $(Et_2SB)_{23}$-*b*-$(MAA)_{49}$ monolayer on the heavy water surface with various NaCl concentrations in subphase. The solid lines are the best fit by the 3-box model. The profile for 1M NaCl could not be fitted. (Copyright ACS with permission)

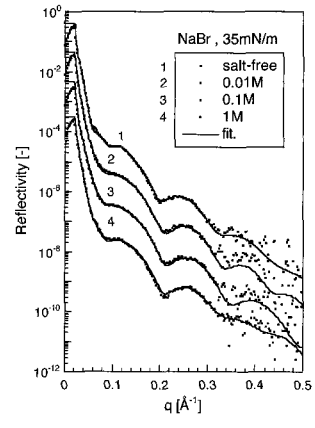

Fig. 3 XR profiles for $(Et_2SB)_{23}$-*b*-$(MAA)_{49}$ monolayer on the water surface with various NaCl concentrations in subphase. The solid lines are the best fit by the 3-box model. The profiles are shifted downward for clarity.

As the first step to solve this paradox, we performed XR and NR measurements for the same polymer monolayer with NaBr as an added salt. Figures 3 and 4 show the XR profiles and the density profiles normal to the water surface for $(Et_2SB)_{23}$-*b*-$(MAA)_{49}$ monolayer on the water surface at 35mN/m under 0M, 0.01M, 0.1M, and 1M NaBr in the subphase conditions, which were the same as in NaCl experiments. These profiles are essentially very similar to those for NaCl as an added salt evaluated by XR (see Figures 2 and 3 in ref.[8], which means that almost the same nanostructure of the monolayer both in NaCl and NaBr systems. In addition, this fact also means that Cl^- and Br^- ions have almost no contribution difference to XR profiles.

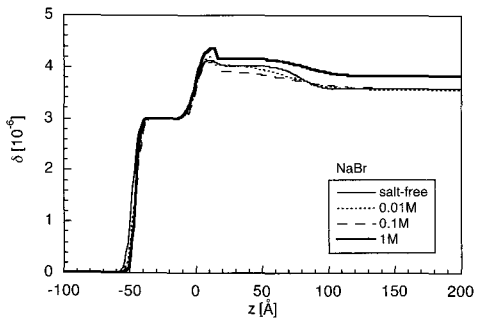

Fig. 4 Density profiles for $(Et_2SB)_{23}$-*b*-$(MAA)_{49}$ monolayer on the water surface with various NaBr concentrations in subphase. δ is defined by n=1-δ-iβ with n the refractive index, which is almost proportional to an electron density.

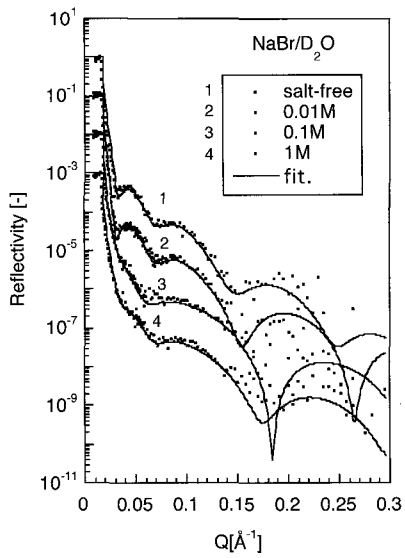

Fig. 5 NR profiles for $(Et_2SB)_{23}$-*b*-$(MAA)_{49}$ monolayer on the heavy water surface with various NaBr concentrations in subphase.

5.2 Effect of NaBr Addition

Figure 5 shows the NR profiles for the same system with D_2O as subphase. The solid lines in the figure are the fitting line by a 3-box model. In this case, the profile for 1M NaBr condition was also well fitted by the 3-box model, while that for 1M NaCl could not previously. The obtained density profiles normal to the water surface is shown in Figure 6. Under all the conditions, the monolayer consisted of hydrophobic, carpet and brush layers and all of these are consistent with that for NaCl addition (see Figure 5 in ref.[8]) both by XR and NR.

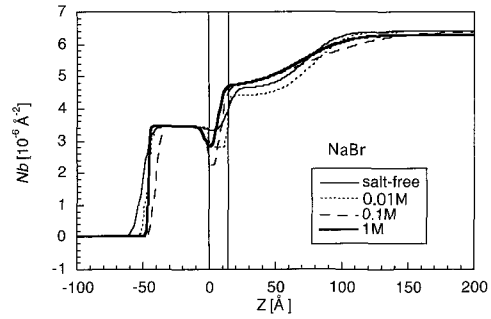

Fig. 6 Scattering length density *Nb* (*N*:the number density, *b* the scattering length) profiles for $(Et_2SB)_{23}$-*b*-$(MAA)_{49}$ monolayer on the heavy water surface with various NaBr concentrations in subphase.

As mentioned in the Introduction, one interesting observation for salt effect on weak polyelectrolyte brush is the change of brush top roughness, i.e., the rougness of the interface between water subphase and brush layer. Our previous study for NaCl system showed that this roughness showed the maximum in a 0.1M NaCl condition. As is clear from Figures 4 and 6, the same phenomenon is also observed for NaBr system. The brush top roughness was influenced by NaBr addition and it becomes maximum at 0.1M NaBr condition. This observation means that the effects of NaCl and NaBr as an added salt are not so different from each other.

The similar effect of NaCl and NaBr as an added salt

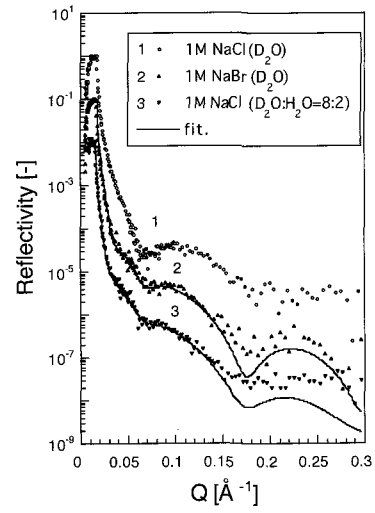

Fig. 7 NR profiles for $(Et_2SB)_{23}$-*b*-$(MAA)_{49}$ monolayer with 1M NaCl on D_2O/H_2O=80/20 (v/v) subphase. Profiles for pure D_2O subphase with 1M NaCl and NaBr are also shown for comparison.

has been confirmed. However, one big difference for these systems is the fact that the NR profile in a 1M NaCl condition could not be fitted by the 3-box model. One possible interpretation for this observation is as follows. For XR measurement, small salt ions did not contribute to the reflectivity profile due to low electron density. For NR, Cl^- ions contribute to the NR profile to some extent, but not Br^- ions, and this becomes substantial with increasing NaCl concentration.

3.3 Contrast variation experiment

To confirm this interpretation, we performed an NR experiment with contrast variation. We used D_2O/H_2O=80/20(v/v) (Nb=5.0x10^{-6}Å^{-2}) as a subphase to eliminate the contribution of Cl^- ions. The NR profile obtained is shown in Figure 7 together with those for a pure D_2O system with 1M NaCl and NaBr. The density profiles evaluated are shown in Figure 8. Even under 1M NaCl condition, NR profile was well fitted by 3-box model when D_2O/H_2O=80/20(v/v) was used as subphase. In addition, the nanostructure of the monolayer is the same for NaBr/D_2O system as shown in Figure 8. This means that the contribution from Cl^- ions to NR profile was eliminated by the contrast matching technique. In other words, the origin of disagreement with 3-box model was contribution of Cl^- ions. This means that the NR profile in a 1M NaCl system contains Cl^- ion contribution, so the small ion distribution can be evaluated by analyzing this NR data.

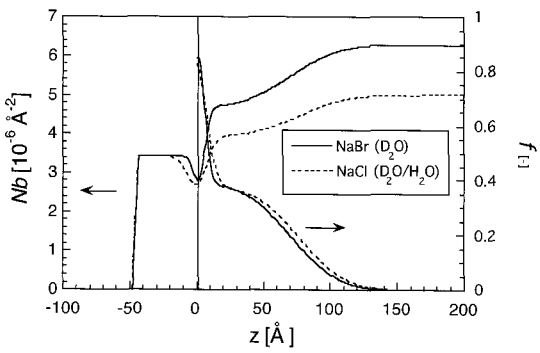

Fig. 8 Scattering density profiles for $(Et_2SB)_{23}$-*b*-$(MAA)_{49}$ monolayer in 1M NaCl on D_2O/H_2O=80/20 (v/v) subphase. The nanostructure is the same as that in a NaBr/D_2O system. f is the volume fraction of hydrophilic chains in the brush layer.

Figure 9 shows the fitting result for NR profile with 1M NaCl as an added salt. The "best" fit by 3-box model was also shown for comparison. As clearly understood from this figure, the fringe height in a 1M NaCl system could not be well reproduced although the fringe position and profile could be to some extent. We have performed a fitting with the model taking the imhomogeneous small ion distribution into account in addition to the 3-box model, i.e., hydrophobic, carpet and brush triple layer structure. A good agreement with the experimental profile was obtained as shown by the solid line in Figure 9.

Figure 10 shows the scattering length density profile obtained from the fitting procedure for Figure 9. The fitting parameters are summarized in Table I. The best fit for NaBr system with 3-box model is also shown. The nanostructure of the monolayer itself is almost the same for these two systems as easily understood by the density profiles in Figure 10. However, the density profile for NaCl system has additional, the fourth layer; High-density layer with about 20Å thickness is located just beneath the carpet layer. Since this layer is not found for NaBr system, this should be the layer in which Cl^- ions are concentrated.

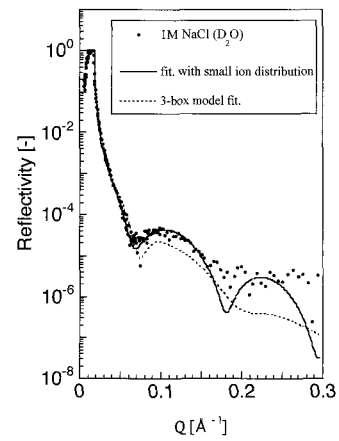

Fig. 9 Fitting result of NR profile for $(Et_2SB)_{23}$-*b*-$(MAA)_{49}$ monolayer with 1M NaCl on D_2O subphase. Dots are experimental data and the solid line is the fitting by the 3-box model taking the inhomogeneous small ion distribution into account. The dotted line is the "best" fit by simple 3-box model.

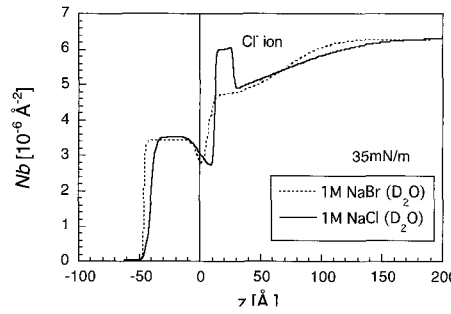

Fig. 10 Scattering density profiles for $(Et_2SB)_{23}$-*b*-$(MAA)_{49}$ monolayer with 1M NaCl and NaBr on D_2O subphase. The profile for NaBr system shows only monolayer nanostructure, while that for NaCl system shows an existence of concentrated Cl^- ion layer just beneath the carpet layer.

The reason why this kind of small anion concentrated layer is formed is not clear at this stage. However, by this systematical study, it is fair to think that there is no doubt that this kind of layer exists. For the correct understanding of this phenomenon, it is necessary to know the location of small cations, which are Na^+ ions and are invisible both by XR and NR in this study. By a similar method as this study, i.e., by using other cations

and applying contrast variation technique of NR, such information will be elucidated. This kind of experiment is our further target.

One may note that *Nb* value inside the "Cl^- ion concentrated layer" is anomalously high. It is almost comparable to that for subphase (1M NaCl in D_2O) and this might be physically impossible when we consider the scattering length density values for Na^+ (Nb=5.55x10^{-6}Å^{-2}), Cl^- ions and D_2O (6.38x10^{-6}Å^{-2}). This might be true, so we think that the density profile model in Figure 10 is the most simple model which can reproduce NR profile in Figure 9 with satisfactory agreement. The real situation might be that the Cl^- layer is more damped, i.e., lower peak top density with larger roughness. However, the statistics of NR data in Figure 9 prevents us to evaluate the detailed nanostructure.

Table I Nanostructure of $(Et_2SB)_{23}$-*b*-$(MAA)_{49}$ monolayer with 1M NaCl and NaBr on D_2O subphase at 35mN/m evaluated by NR

Salt	NaCl			NaBr		
Layer No.	*Nb* [10^{-6}Å^{-2}]	*d* [Å]	σ [Å]	*Nb* [10^{-6}Å^{-2}]	*d* [Å]	σ [Å]
1	3.43	40	3	3.43	45	1
2	2.30	12	8	1.87	6	4
3-1	4.00	1	1			4
3-2	5.60	15	1			
4	4.40	37	1	4.68	65	
5	6.31		55	6.28		28

layer 1 :hydrophobic layer, 2:carpet layer, 3:newly found layer for NaCl system, 4:brush layer, 5:subphase
Nb:scattering length density for each layer, *d*: thickness, σ: interface roughness between each layer

The estimation of small ion distribution near macroions by neutrons is not common but not nil. For example, Sumaru et al. [24], determined counterion distribution around ionic micelle by small-angle neutron scattering, and they showed that it followed the Poisson-Boltzmann behavior. In this study, we have found the small ion concentrated layer in the brush layer. The ion concentration in the polyelectrolyte brush is very high and special. This unique environment might be the origin of our curious observation in this study.

In the present study, we did not consider the effect of surface concentration on the isotope effect. However, since we obtained satisfactory agreement between reflectivity data and model calculation, we concluded that this effect is not significant in the present case. In addition, our observation is specific to a NaCl system but not a NaBr system, which means essentially no relationship to this effect.

3.4 Estimation of brush top roughness

Finally, we estimated the roughness function of the brush top. As described previously, the large and characteristic change of the brush top roughness is one of the unique observations on the salt effect for a weak polyelectrolyte brush. Since the contrast between the brush layer (hydrogenated polymer + D_2O) and subphase (D_2O) is higher than that for XR (i.e., an electron density difference), this kind of estimation becomes possible by the NR technique.

We used three typical functions for the brush top roughness as follows.

(i) Error Function

$$F(z)=\int_0^z C\left(\frac{1}{B\sqrt{2\pi}}\right)\exp\left(\frac{-(z-A)^2}{2B^2}\right)dz \qquad (1)$$

where A is the position of the interface, B the interface roughness, and C the density difference between two layers which form interface.

(ii) Parabolic Function

$$F(z)=A+B\left((z-C)^2\right) \qquad (2)$$

where A is the Nb value at the interface, B the interface roughness, and C the position of the interface.

(iii) Hyperbolic Tangent

$$F(z)=\frac{\exp\left[B(z-D)\right]-\exp\left[-B(z-D)\right]}{\exp\left[B(z-D)\right]+\exp\left[-B(z-D)\right]}C+A \qquad (3)$$

where A is the Nb value at the interface, B the interface roughness, C the density difference between two layers which form interface, and D the position of the interface.

Figure 11 shows the fitting of NR profile for 35mN/m on D_2O without salt by using three different functions for brush surface roughness. Other nonstructural parameters of the monolayer were kept constant. The corresponding density profiles were shown in Figure 12. Although the difference of fitting quality in Figure 11 is not so distinct, as a whole, the Gaussian (Error function) could reproduce the NR profile in the best. At least for our present data, the Error function is the best function to describe the brush top roughness.

4.CONCLUSION

The small ion distribution in the brush layer in a weak acid amphiphilic diblock copolymer, $(Et_2SB)_{23}$-*b*-$(MAA)_{49}$, monolayer on the water surface was evaluated by the NR technique. By XR measurements with NaCl and NaBr as an added salt for water subphase, the nanostructure of the monolayer, which consists of a hydrophobic, carpet, and brush layer, could be estimated and no specific contribution from added salt ions to XR profile was noticed. Also for the NR profile with NaBr in the D_2O subphase, no contribution from small ions was found. However, the NR profile in 1M NaCl on D_2O could not be fitted by the same structural model. By contrast variation NR measurement, this disagreement was found to be due to the contribution of Cl^- ions to the NR profile. Taking into account the inhomogeneous Cl^- ion distribution in the brush layer, it was suggested that Cl^- ions form a concentrated layer just beneath the carpet layer with about 20Å thickness. The Gaussian function was found to be the most suitable function to describe the brush top roughness.

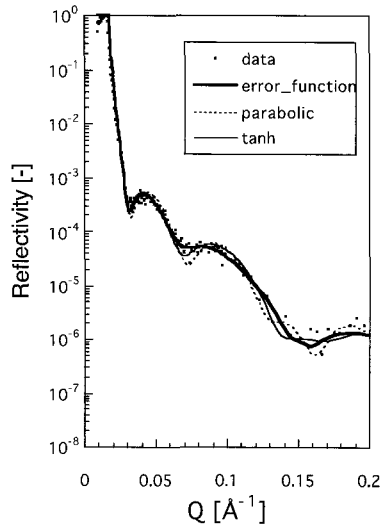

Fig. 11 Fitting result of NR profile for $(Et_2SB)_{23}$-*b*-$(MAA)_{49}$ monolayer on D_2O subphase at 35mN/m with three different roughness functions for the brush top.

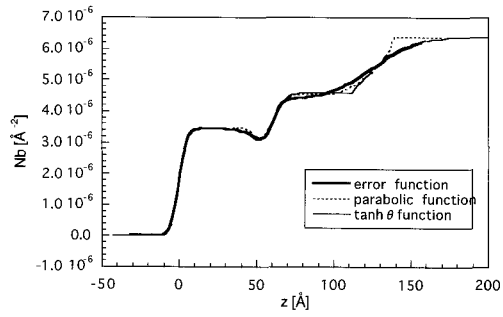

Fig. 12 Scattering density profiles for $(Et_2SB)_{23}$-*b*-$(MAA)_{49}$ monolayer on D_2O subphase at 35mN/m evaluated by fitting of NR profile with three different roughness functions for the brush top.

ACKNOLEDGEMENT

This work was supported by a grant-in-aid for Scientific Research from the Ministry of Education, Culture, Sports, Science and Technology of Japan, to whom our sincere gratitude is due. This work was also supported by the 21st Century COE Program, COE for a United Approach to New Materials Science.

REFERENCES

[1] P.G.De Gennes, P *Macromolecules*, **13**, 1069 (1980).
[2] S.T.Milner, S. T. *Science*, **251**, 905 (1991).
[3] A.Halperin, M.Tirrell, T.P.Lodge, *Adv. Polym. Sci.*, **100**, 31 (1992).
[4] R.C.Advincula,W.J.Brittain, K.C.Caster, J.Rühe (Eds.) *"Polymer Brushes"* Wiley, 2004.
[5] I.W.Hamley,*"Block Copolymers in Solution: Fundamentals and Applications"* Wiley, chapter5, 2005.
[6] H.Ahrens, S.Förster, C.A.Helm, *Phys. Rev. Lett.* **81**, 4172 (1998).
[7] E.Mouri, Y.Furuya, K.Matsumoto, H.Matsuoka, *Langmuir*, **20**, 8062 (2004).
[8] E.Mouri,P.Kaewsaiha,K.Matsumoto, H.Matsuoka, N.Torikai, *Langmuir*, **20**, 10604 (2004).
[9] E.Mouri, K.Matsumoto, H.Matsuoka, N.Torikai, *Langmuir*, **21**,1840 (2005).
[10] P.Kaewsaiha, K.Matsumoto,H.Matsuoka, *Langmuir*, **20**, 6754 (2004).
[11] P.Kaewsaiha,K.Matsumoto, H.Matsuoka, *Langmuir*, **23**, 20 (2007).
[12] P.Kaewsaiha,K.Matsumoto, H.Matsuoka, *Langmuir*, **21**, 9938 (2005).
[13] H.Matsuoka,Y.Furuya,P.Kaewsaiha, K.Matsumoto, *Langmuir*, **21**, 6845 (2005).
[14] H.Matsuoka,Y.Furuya,,P.Kaewsaiha,K.Matsumoto, *Macromolecules*, in press.
[15] Y.Suetomi, P.Kaewsaiha, K.Matsumoto, H.Matsuoka,, *Polym. Prepr. Jpn.*, **55**, 4373 (2006).
[16] K.Matsumoto, C.Wahnes, E.Mouri, H.Matsuoka, H.Yamaoka, *J.Polym.Sci. A, Polym.Chem.*, **39**, 86 (2001).
[17] H.Matsuoka, E.Mouri, K.Matsumoto, *Rigaku Journal*, **18**, 54 (2001).
[18] N.Torikai, M.Furusaka, H.Matsuoka, Y.Matsushita, M.Shibayama, A.Takahara, M.Takeda, S.Tasaki, H.Yamaoka, *Applied Physics A*, **74[suppl]**, S264 (2002).
[19] E.Mouri, K.Matsumoto, H.Matsuoka, *J.Appl.Cryst.* **36(3)**, 722 (2003).
[20] E.B.Zhulina, O.V.Borisov, V.A.Priamitsyn, *J. Colloid Interface Sci.*, **137**, 495 (1990).
[21] E.B.Zhulina,T.M.Birshtein,O.V.Borisov, *Macromolecules*, **28**, 1491 (1995).
[22] O.V.Borisov, T.M.Birshtein, E.B.Zhulina, *J. Phys. (Paris)*, **1**, 512 (1991).
[23] E.B.Zhulina, O.V.Borisov, T.M.Birshtein, *Macromolecules*, **32**, 8189 (1999).
[24] K.Sumaru, H.Matsuoka, H.Yamaoka, G.D.Wignall, *Phy.Rev.E*, **53**, 1744 (1996).

(Received December 9, 2006;Accepted February 8, 2007)